Influence of Poly(ether imide) on the Free Volume Hole Size and Distributions in Poly(ether ether ketone)

R. Ramani, S. Alam

Polymer Science Division, Defence Materials and Stores Research and Development Establishment (DMSRDE), Kanpur 208 013, India

ABSTRACT: Blends of poly(ether ether ketone) (PEEK) and poly(ether imide) (PEI) were examined for their miscibility at the nanoscopic level using positron annihilation lifetime spectroscopy (PALS) and modulated differential scanning calorimetry (MDSC). The free volume results obtained from PALS reveal that PEEK and PEI exhibit high degree of miscibility showing interlamellar segregation when the PEI content in the blend is $\geq$50%. Although the average free volume sizes of PEEK and PEI are nearly same, a clear distinction could be made from their size distribution. The free volume of PEI is found to be narrow as compared with PEEK. Also, herein, we provide the first evidence of the influence of interlamellar segregation on the free volume distribution in a polymer blend. The crystalline structure of the blend was studied by X-ray scattering and the surface morphology was examined by scanning electron microscopy (SEM). The MDSC results indicate the presence of a possible rigid amorphous fraction (RAF) and corroborate the positron lifetime and X-ray scattering results. © 2012 Wiley Periodicals, Inc. J Appl Polym Sci 125: 3200–3210, 2012

Key words: poly(ether ether ketone); poly(ether imide); miscible blend; free volume distribution; positron lifetime; modulated DSC

INTRODUCTION

The polymers poly(ether ether ketone) (PEEK) and poly(ether imide) (PEI) are high-performance polymers. The PEEK is a semicrystalline thermoplastic having good chemical resistance and superior mechanical properties. It is suitable for use as a matrix material in the preparation of thermoplastic composites owing to its good adhesion to glass and carbon fibers.[1,2] Since the glass transition temperature (T_g) of PEEK is ca. 145°C, the modulus of these materials decreases above this temperature.[3] On the other hand PEI is an amorphous polymer with comparatively high T_g of around 215°C.[2,3] But, PEI has a lower chemical resistance than that of PEEK and cannot be used above its T_g.[3] Blending of these two polymers combines the complimentary properties of both of them and hence PEEK/PEI blends have been the subject of several investigations for more than two decades.[1–9] As of now, it is only known that PEEK and PEI forms a miscible blend,[1,3,6,9] but a thorough understanding on the extent of miscibility at the nanoscopic level of this high-performance polymer blend is still lacking.

The conventional means of determining the miscibility in a polymer blend system is by using differential scanning calorimetry (DSC) or dynamic mechanical analysis (DMA) or dielectric analysis (DEA).[5,6,9,10] Not so frequently, even solid-state NMR is being used to study the miscibility of polymer blends.[11] In a DSC, the existence of a single T_g between those of the constituent polymers has been accepted as a general criterion for miscibility while two T_g s at the original position represents an immiscible blend.[10,12] According to Kammar et al.,[13] the typical domain size sensitivity of conventional DSC to phase-separated polymeric materials is ca. 50 nm. But, the identification of T_g using conventional DSC is influenced by any additional processes that takes place near the glass transition and often provides a weak indication of T_g.[14]

The introduction of modulated differential scanning calorimeter (MDSC) has permitted to understand the polymer miscibility in a better way compared with conventional DSC.[15,16] It is important to note that the polymer blends that are judged miscible based on conventional DSC have shown two calorimetric T_g s based on heat capacity (C_p) results obtained from MDSC.[12,17] The results of these experiments have made clear that the indication of a single T_g by DSC is not a universal feature to judge the polymer miscibility.[12] The reversing signal in a MDSC provides an excellent resolution of the glass transition by separating the heat capacity from the nonreversing processes such as enthalpy relaxation and crystallization.[16] Hence, it is useful to explore the T_g from the reversible C_p (C_p^{rev}) vs. temperature

plot as well as from the temperature derivative of C_p^{rev}; (dC_p^{rev}/dT) vs. temperature plot.[14,18] The T_g determined by this method has a high resolution compared with DSC and DMA and thereby helps in better judgment of polymer blend miscibility.[12,14,15]

Another approach to understand the polymer blend miscibility at the nanoscopic level is by studying the free volume.[19] The free volume is an intrinsic element of the amorphous phase of a polymer resulting from incomplete packing.[20] If there is a favorable interaction between the two components of a polymer blend, generally a reduction in free volume is observed than that is predicted by a simple additivity rule (negative deviation) revealing that the blend is miscible. A positive deviation from additivity indicates an immiscible blend. Therefore, studies on free volume holes have been successfully used for determining whether the blends are miscible or not at the nanoscopic level.[19,20,21] Furthermore, the evaluation of free volume distribution in the blends also provides more valuable information about its structure and miscibility.[10,19] In case of a miscible blend, single Gaussian-like distribution of free volume between those of the two original constituents is expected.[10,19,22,23] On the other hand, an immiscible blend is expected to exhibit a broader distribution as a consequence of different phases and interphases present in the blend and the distribution pattern would be unsymmetric. Thus, finer details on the miscibility aspects of the polymer blend is possible by studying the free volume hole distribution.[10,19,22,23]

The study on free volume is of crucial importance for polymers because it influences the molecular motion and physical properties of polymers. This in turn will have an influence on their mechanical and visco-elastic properties.[16,24] The positron lifetime annihilation spectroscopy (PALS) is used for characterizing the free volumes in polymers for decades[25] and in the recent past, it has also been used for studying the polymer blends.[10,19,21,23] From PALS measurement, one can get information regarding the average free volume size, their concentration, as well as free volume distribution.[10,19,23] A brief description of PALS is provided in the experimental section.

Although, PEEK/PEI blend has been the subject of several investigations,[1–9] the free volume studies have been limited to the constituent polymers PEEK and PEI alone.[20,25,26] Despite the prominent utility of PEEK and its blends in aerospace applications,[27] to the best of our knowledge, there are no scientific works to date that clarifies the extent of miscibility of PEEK/PEI blend at the nanoscopic level in terms of change in free volume size and distribution. Here, we provide a thorough investigation in this regard using PALS method. The MDSC results supplement the positron lifetime results. Additionally, the crystalline structure of the blends was studied by X-ray
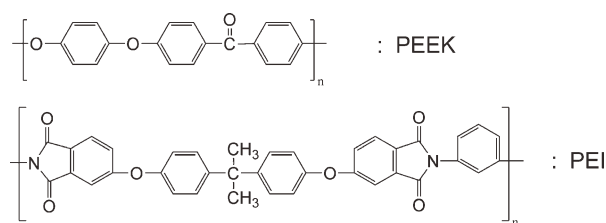
Scheme 1 Chemical formulas of PEEK and PEI.

Scattering and the morphology of the blends was examined by scanning electron microscopy (SEM).

EXPERIMENTAL

Sample preparation

Granular PEEK-grade Victrex 450G having melt viscosity of 350 pa.s at 400°C, molecular weight of 40,000 g/mol, and a polydispersity of 2.8 was purchased from Victrex, UK. The PEI-grade Ultem 1000 with molecular weight of 30,000 g/mol, polydispersity of 2.5, and intrinsic viscosity of 0.47 dL/g was obtained from General Electric Plastics, Europe. Blends with weight ratios of PEEK/PEI 100/0, 90/10, 80/20, 70/30, 50/50, 30/70, and 0/100 were prepared by melt mixing. The blends were processed and prepared under identical conditions to minimize the microstructural changes that may arise due to processing conditions. Details of the blend preparation can be found in our recent report.[9] These blends are designated respectively as P_0, P_{10}, P_{20}, P_{30}, P_{50}, $P_{70,}$ and P_{100} (where the subscripts represent the wt % of PEI). To check the reproducibility of measurements (wherever needed), samples from the same batch was used. The chemical structure of the PEEK and PEI is shown in Scheme 1.

Characterization

Modulated differential scanning calorimetry

Although the main aim of the work is to understand the free volume size and its distribution in PEEK/PEI blend and thereby to check the extent of miscibility of this blend at the nanoscopic level, we have first performed MDSC measurements to elucidate that this blend has single T_g based on the thermal profiles of reversible C_p (C_p^{rev}) and its temperature derivative (dC_p^{rev}/dT).

The MDSC was performed using an indium- (temperature) and sapphire- (heat capacity) calibrated Q200 (TA instruments) in nitrogen atmosphere (flow rate = 50 mL/min). The instrument is equipped with a refrigerated cooling system and has a temperature accuracy of ± 0.1°C. The cell constant calibration was also obtained from the indium standard.

Samples of ∼6 mg were weighed and sealed in aluminum sample pans and were heated above their melting temperature for 5 min in a conventional manner to erase the thermal history. The modulation temperature amplitude was kept small (0.32°C) relative to the underlying heating rate (2°C/min), so that no local cooling during the standard MDSC scan (heating-only) and the modulation period was kept as 60 s. The peak temperature of dC_p^{rev}/dT is equated to the middle of the step-change in C_p^{rev} curve.

Positron annihilation lifetime spectroscopy

The PALS is a powerful technique to evaluate the free volume size due to the unique localization of positron and positronium in open spaces.[20,25,28,29] In PALS method, positrons are emitted from [22]Na radioactive source and transferred into the polymer under study. When positron enters a polymer sample, it can annihilate as a free positron in a polymer with a lifetime of about 0.3–0.5 ns. The positron can also form a bound state called positronium (Ps) that can exist in two spin states; ortho-positronium (o-Ps) and para-positronium (p-Ps). In p-Ps, the spins of the positron and electron are antiparallel, and has an intrinsic lifetime of around 0.125 ns in vacuum while in o-Ps, the spins of the electron and positron are parallel and has an intrinsic lifetime of 142 ns in vacuum.[25,29] In condensed matter, however, the positron of o-Ps may annihilate with one of the surrounding electrons having opposite-spin, by the process of pick-off annihilation. In this process, the o-Ps lifetime gets reduced to few nanoseconds. It is this o-Ps pick-off annihilation lifetime (τ_3) that provides the average size of the free volume and its intensity I_3 represents the o-Ps formation probability.[20,29]

The PALS measurements were performed in air medium at room temperature using the "fast-fast" coincidence system of the Department of Studies in Physics, University of Mysore, Mysore, India. The spectrometer has a time resolution of 220 ps based on a ^{60}Co source with energy windows set to [22]Na events and more details on this instrument can be found elsewhere.[21] The measurements were repeated at least thrice at each level of PEI content in the blend and reproducible results were obtained. Each spectrum was collected with sufficient counts so as to obtain statistically agreeable results. Analysis of the positron lifetime spectra were performed by two evaluation methods, finite-term lifetime analysis using PATFIT-88 program[30] and continuous lifetime distribution analysis by MELT program.[31] Three component analyses gave better convergence over two and four component analysis with PATFIT-88 and resulted to mean life-

times and intensities. The spectra when analyzed using MELT yielded distribution of the three life-times. Since the o-Ps pick-off annihilation characteristics (τ_3, I_3) were the main parameters of interest for polymeric materials, only they will be the focus of discussion in this article.[20]

To calculate the average hole size from the o-Ps lifetime (τ_3), we have used the so-called "standard model" based on Tao-Eldrup equation where it is assumed that o-Ps is confined in an infinitely deep spherical potential well[32,33] of radius R. The relation between τ_3 and R is given by

$$\tau_3 = 0.5[1 - (R/R_{\mathrm{o}}) + (1/2\pi)\ \sin\ 2\pi(R/R_{\mathrm{o}})]^{-1}\ \ \mathrm{ns}$$

(1)

where the prefactor 0.5 ns is the spin-averaged Ps annihilation lifetime and $R_{\mathrm{o}} = R + \Delta R$ with $\Delta R = 0.1656$ nm is the fitted electron layer thickness obtained by fitting eq. (1) to positron lifetime values measured in systems of known hole sizes.[20,25] Using this value of R, the average free volume size at different compositions of the blend was found as $V_{f3} = (4/3)\pi R^3$. The o-Ps intensity I_3 depends on the probability of o-Ps formation and is often considered by many authors that it may be proportional to the concentration of free volume holes.[20,21] The free volume fraction F_v in polymer can be estimated using the relation $F_v = CI_3V_{f3}$ where the parameter C is termed as structural constant that can be obtained from other experiments.[20,24] However, a precise determination of C becomes difficult for polymer blends with semicrystalline constituents because, the thermal history varies with the degree of crystallinity.[24] Because of uncertain C parameter for the present blend system, the F_v here is expressed as the relative fractional free volume $(F_{vr}) = V_{f3}.I_3$[21,26] and is used to discuss the results. The relative density (ρ) of the blends were determined according to ISO 1183 : 1987 as reported.[8]

Small angle X-ray scattering

In the X-ray scattering experiments, the samples were sealed between two thin Kapton© foils and the raw intensity data were corrected for background scattering. The SAXS system consists of a 2D area detector (Bruker AXS) and a Bruker MICROSTAR rotating anode X-ray source with Montel optics (Cu K_α radiation, $\lambda = 1.54$ Å). The beam was further collimated with four sets of four-blade slits resulting in a beam of about 1 mm × 1 mm at the sample position. A distance of about ∼ 0.45 m was maintained between the sample and the detector. The magnitude of the scattering vector is given by $q = (4\pi/\lambda)$
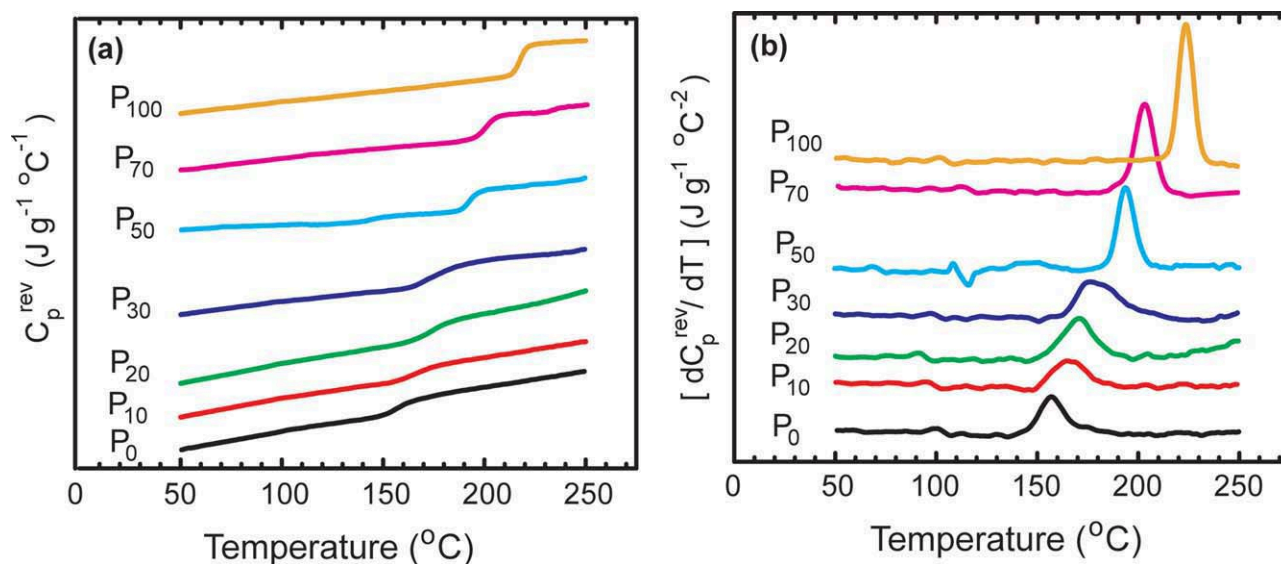
Figure 1 The MDSC plots for different ratios of PEEK/PEI upon heating showing (a) C_p^{rev} versus temperature and (b) $[dC_p^{rev}/dT]$ versus temperature curves for various compositions of PEEK/PEI blend. The curves have been displaced vertically for clarity. [Color figure can be viewed in the online issue, which is available at wileyonlinelibrary.com.]

Sinθ, where θ is the half-scattering angle. The q range was calibrated with silver behenate standard.

Wide angle X-ray scattering

The WAXS patterns were collected with a Rigaku X-ray machine with a rotating anode source (Cu K$_\alpha$ radiation, $\lambda = 1.54$ Å). The X-ray beam was focused on the detector and monochromated using a totally reflecting mirror and a Si (111) crystal giving an X-ray beam size of about 2 mm × 2 mm on the sample surface. The scattered radiation was detected with an image plate detector MAR345. The q range was calibrated with silver behenate and Si-powder standards.

Scanning electron microscopy

To further visualize the phase homogeneity, the surface morphology of the blends was examined using a Carl Zeiss Supra 40 VP field emission scanning electron microscope with 20 kV accelerating voltage. The samples were sputter coated with gold on the viewing surface to enhance its conductivity.

RESULTS AND DISCUSSION

MDSC results

First we will analyze the possible existence of multiple T_gs in this PEEK/PEI blend from the MDSC results. We have recently reported a detailed thermal behavior of this blend using conventional DSC[9] and hence here we will focus only on the miscibility aspect of this blend in terms of identifiable T_gs. For

this, C_p^{rev} and its temperature derivative (dC_p^{rev}/dT) are plotted against temperature (30–250°C) and the same are shown in Figure 1(a,b), respectively. The quantitative results from MDSC are tabulated in Table I.

All the samples showed T_g during heating and the values of T_g of these blends increased with the increasing PEI content.[9] The dC_p^{rev}/dT vs. temperature curves shows only one peak associated with the change near glass transition for all the blend compositions [see Table I and Fig. 1(b)] indicating single T_g in them.[15] This rule out immiscibility at any proportions in the blend. The T_g values obtained for various blend compositions are close to the values reported using conventional DSC[9] and the small difference in the values could be attributed to the difference in heating rate used (2°C/min for MDSC as against 20°C/min in conventional DSC).

When amorphous PEI is added to semicrystalline PEEK and upon crystallization of the latter, PEI is

TABLE I
MDSC Results of PEEK/PEI Blend

Sample	MDSC		DSC[a]		
	T_g (°C)	ΔC_p (J g^{-1} °C^{-1})	T_g (°C)	T_m (°C)	ΔH_m (J g^{-1})
P_0	152	0.093	155	341	31.9
P_{10}	161	0.1008	164	339	27.9
P_{20}	166	0.1107	168	339	25.8
P_{30}	170	0.1171	172	338	21.4
P_{50}	185	0.1172	188	332	5.2
P_{70}	198	0.1479	200	332	1.9
P_{100}	218	0.1822	220	–	–

[a] Extracted from results published in Ref. 9.

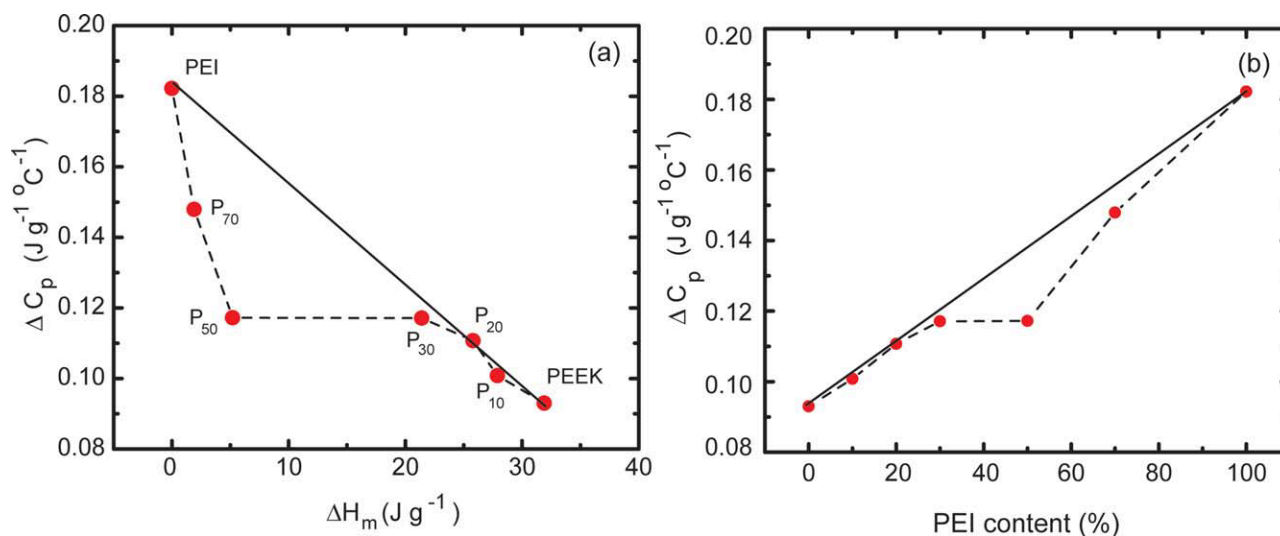**Figure 2** Variation of ΔC_p with (a) ΔH_m and (b) PEI content for various compositions of PEEK/PEI blend. [Color figure can be viewed in the online issue, which is available at wileyonlinelibrary.com.]

rejected into the amorphous domains of PEEK. Hence, there is a progressive enrichment of PEI in the amorphous regions of PEEK.[7] This leads to a change in the composition of the amorphous phase of PEEK. Thus, the increase in T_g of the blend with increase in PEI composition implies increase of mobility restrictions brought to the amorphous segments of PEEK. In our previous study with the conventional DSC,[9] we have observed a significant change in melting temperature (T_m) and the melting enthalpy (ΔH_m) when the PEI content in the blend is 50% (see Table I). On the basis of the previous work by other research groups on this blend,[4,6] and from our combined thermogravimetric analysis (TGA) kinetics and DSC results,[9] we had proposed interlamellar segregation of PEI chains into the PEEK lamellae when the PEI content in the blend is ≥50%. In this work, we provide more experimental evidences to strengthen this concept. This kind of interlamellar inclusion of PEI is most likely due to the tendency of the PEEK lamellae that prefers a close parallel growth. It is to be noted that such semicrystalline aromatic polymers can tolerate the interlamellar inclusion to certain extent which is probably related to the increased stiffness of the aromatic chains.[6] If the PEI chains are segregated in the interlamellar regions of PEEK, these chains should behave more like rigid amorphous fraction (RAF), in which that fraction of amorphous chains will only have restricted molecular motion (owing to its sandwich arrangement between the crystalline domains) and do not contribute to jump in heat capacity at T_g.[34]

To understand the possible presence of RAF and hence the interlamellar segregation in this blend, a plot of change in heat capacity at $T_g(\Delta C_p)$ is made against melting enthalpy (ΔH_m) values obtained from the total heat flow [Fig. 2(a)]. The addition of

PEI to PEEK not only increases the T_g of PEEK, but also decreases its crystallization behavior as revealed by the ΔH_m value (see Table I). The decrease in crystallinity of PEEK is also confirmed by the X-ray scattering results, that will be discussed later. If all the parts of the amorphous domains participate in the T_g, the plot of ΔC_p vs. ΔH_m should show a linear behavior.[35] Interestingly, the plot showed a linear behavior up to 30% of PEI content (sample P_{30}) and beyond which the trend became nonlinear [see Fig 2(a)]. In fact, a large deviation from linearity can be observed when the PEI content in the blend is ≥50%, thus giving an indication for the presence of RAF in the blend at this composition of PEI and onwards.

Now, having seen the variation of ΔC_p with crystalline content (ΔH_m), it is curious to understand its change with amorphous content (% of PEI) in the blend. From the plot of ΔC_p vs. PEI content in the blend [Fig. 2(b)], we can see that the ΔC_p increases with the increase of PEI content, but its value is little less than the ΔC_p expected on the basis of simple additivity rule. This reveals that the excess heat capacities of mixing have negative values and is a common trend observed in miscible blends.[36] However, a careful observation of this curve also reveals that more negative deviation of ΔC_p from linearity is observed when the PEI content is ≥50% that could be attributed to greater extent of miscibility, because of interlamellar segregation.

Positron lifetime results

Composition dependence of free volume

The positron lifetime results obtained from PATFIT and MELT analysis are tabulated in Table II. Figure

TABLE II
Density and PALS Results of PEEK/PEI Blend

Sample	ρ (g/cm^3)	Patfit analysis				Melt analysis		
		τ_3 (ns)[a]	I_3 (%)[a]	V_{f3} (Å)^3	F_{rv} (%)	τ_3 (ns)	I_3 (%)	V_{f3} (Å)^3
P_0	1.302	1.690 ± 0.032	4.7 ± 0.2	69.7 ± 2.2	3.28	1.716	4.5	71.9
P_{10}	1.300	1.682 ± 0.024	5.2 ± 0.2	69.0 ± 1.7	3.59	1.704	5.7	70.9
P_{20}	1.298	1.713 ± 0.023	7.1 ± 0.2	71.6 ± 1.7	5.08	1.738	6.8	73.8
P_{30}	1.297	1.782 ± 0.018	7.0 ± 0.2	77.7 ± 1.3	5.44	1.806	6.6	79.8
P_{50}	1.293	1.776 ± 0.013	8.3 ± 0.2	77.2 ± 1.0	6.41	1.796	9.2	78.9
P_{70}	1.290	1.765 ± 0.012	11.9 ± 0.2	76.2 ± 0.9	9.08	1.789	12.6	78.3
P_{100}	1.287	1.703 ± 0.010	20.0 ± 0.2	70.8 ± 0.7	14.16	1.690	20.8	69.7

[a] The uncertainties in τ_3 and I_3 values are the standard deviations.

3(a) shows the plot of o-Ps lifetime (τ_3) and the average free volume size with PEI content while Figure 3(b) depicts the change in o-Ps intensity (I_3) against PEI content in the blend. The average free volume size remains almost constant (ca. 70 Å^3) when the PEI content is ≤10%. It increases to a value of ca. 78 Å^3 when the PEI content is 30%, and with further addition of PEI, it gradually reverts back close to its original value (ca. 71 Å^3). Generally, it is expected that in a miscible blend, the free volume to decrease with the increase in composition of the other component. However, an increase in free volume in a miscible blend with the change in composition of its other partner is not something new. It has been reported that the free volume behavior of miscible blends may be additive or decrease and is influenced more by segmental conformation and packing than by specific interactions.[37] The decrease in free volume when the PEI content is ≥50% could be due to close packing of PEEK and PEI chains upon interlamellar segregation, thus contributing to greater extent of miscibility.

Although the change in o-Ps lifetime (τ_3) is not that significant, the o-Ps intensity (I_3) shows a prominent change with PEI content [Fig. 3(b)]. For pure PEEK, I_3 is just ca. 4.7% but with the increase in PEI content, the I_3 value also increases gradually and reaches a value of ca. 20% for the pure PEI sample while the density of the sample shows an opposite trend with the increase in PEI content (see Table II). This is because, addition of PEI increases the amorphous content of the blend, and hence the number of free volume regions (I_3) also increases in accordance with the known concept.[16,20] The increased free volume regions results to obvious decrease in density. The I_3 shows a negative deviation from linearity indicating that the blend is miscible[19,21] and the deviation is more when the PEI content in the blend is ≥50%. This means that the local environment probed by o-Ps has been changed significantly at this stage which again goes in agreement with the concept of interlamellar segregation. Our PALS three lifetime component results for pure PEEK and PEI are comparable with their reported values[20,25,26] and the difference in numerical values could be attributed to different grades of PEEK and PEI used.

In a PALS study, apart from change in I_3, the relative fractional free volume (F_{vr}) and the interchain
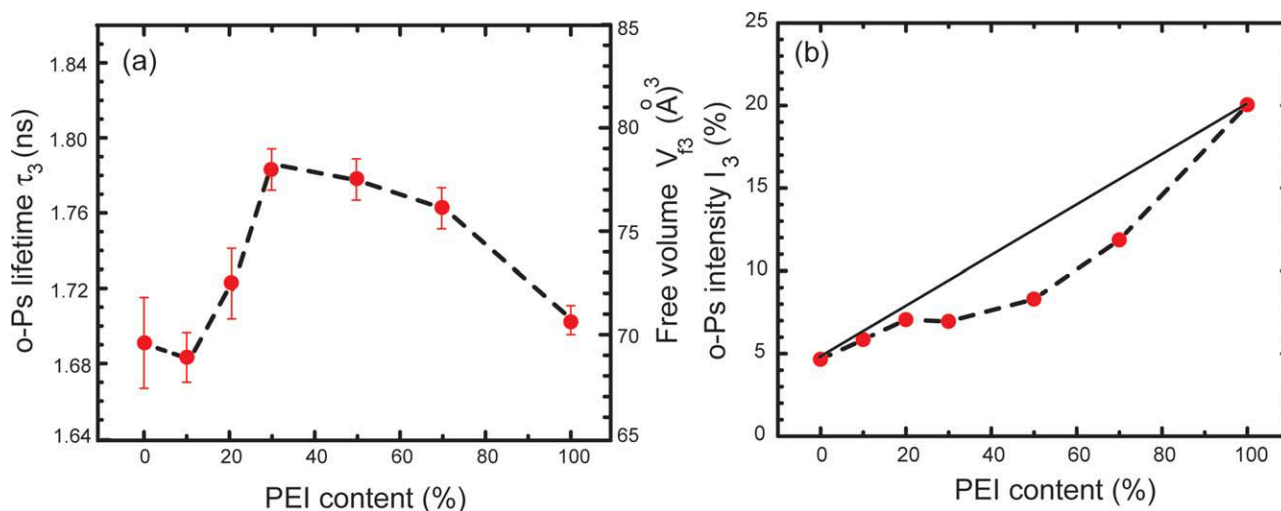

Figure 3 (a) Variation of o-Ps lifetime (τ_3) and average free volume size (V_{f3}) vs. PEI content and (b) Variation of o-Ps intensity (I_3) vs. PEI content. [Color figure can be viewed in the online issue, which is available at wileyonlinelibrary.com.]
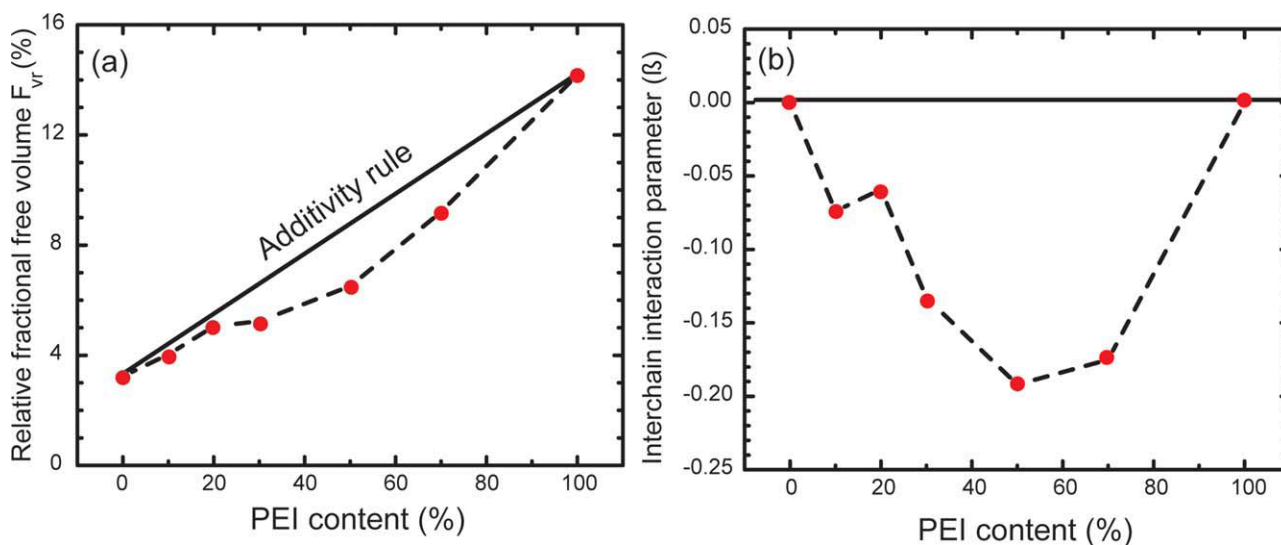
Figure 4 (a) Variation of relative fractional free volume F_{vr} (%) vs. PEI content and (b) Variation of interchain interaction parameter (β) vs. PEI content. [Color figure can be viewed in the online issue, which is available at wileyonlinelibrary.com.]

interaction parameter (β) are the other two parameters that are commonly used to understand the miscibility of polymer blends.[19,21] The variation of F_{vr} with PEI content [Fig. 4(a)] shows a similar trend as that of I_3 implying that the major contribution to the overall change in free volume content is arising from the number of free volumes than from the average free volume size. The large negative deviation of F_{vr} when the PEI content is ≥50% also reveals that the PEEK/PEI blend achieves high degree of miscibility at these compositions.

For a simple binary interchain interaction, one can express the free volume hole fraction of the blend as

$$F_V = F_{V1}\phi_1 + F_{V2}\phi_2 + \beta F_{V1}\phi_1 F_{V2}\phi_2 \qquad (2)$$

where F_{V1}, F_{V2}, ϕ_1, and ϕ_2 are the free volume hole fractions and specific volume fractions of the constituent polymers 1 and 2, respectively and β is a parameter that could be related to the interaction between dissimilar chains. In case of miscible blends, the β parameter is negative.[19,21] The values of β thus calculated from eq. (5) (here instead of F_v we have used their respective F_{vr} values) are plotted against the PEI content [Fig 4(b)]. The value of β attains a minimum (β = −0.18) when the PEI content in the blend is 50% which is again an indication of high degree of miscibility and free volume contraction [Fig. 4(b)]. The contraction of free volume results in decrease of Gibb's free energy which is a general criterion for a miscible blend.[19] From these results, we can conclude that excellent miscibility of PEEK/PEI blends is obtained when the PEI content is ≥50%. However, recent report suggests that β parameter is not sufficient to conclude the extent of miscibility in a polymer blend.[21]

Free volume hole size distribution

In order to further confirm these results on the extent of miscibility, we have obtained the o-Ps lifetime distributions and the associated distribution in free volume hole size for each of these blend compositions using MELT [see Fig. 5(a,b)]. The free volume size distribution point out the heterogeneity of the local environment of the annihilating o-Ps atom. The results obtained from MELT analysis are comparable to those obtained from PATFIT analysis (see Table II) as reported in other polymers.[23,38]

The first striking feature that can be derived from Figure 5(a,b) is that even though both PEEK and PEI have the same average free volume size [see Table II and Fig. 3(a)], their distribution patterns are quite unlike [note that the y-axis scales in Fig. 5(a,b) are different). PEI has a narrow hole size distribution as compared to PEEK implying that the free volume holes in PEI are relatively uniform in size. On comparing the free volume size distributions at different levels of PEI addition, it can be noticed that till the PEI content is <50%, the distribution changes to slightly broad and the two tails stretch out towards smaller and larger size. But, the pattern of symmetric distribution is retained. The small and large hole sizes seems to result from the contribution of possible interfaces between the polymer chains indicating that the extent of miscibility is not the best possible.

The second striking observation from these distribution patterns is that they become narrow when the PEI content in the blend is ≥ 50% [see Fig. 5(b)]. To better appreciate this result, the o-Ps lifetime distribution pattern of the whole blend composition is shown as an inset in Figure 5(b). Such a sudden change in the distribution pattern signifies that there
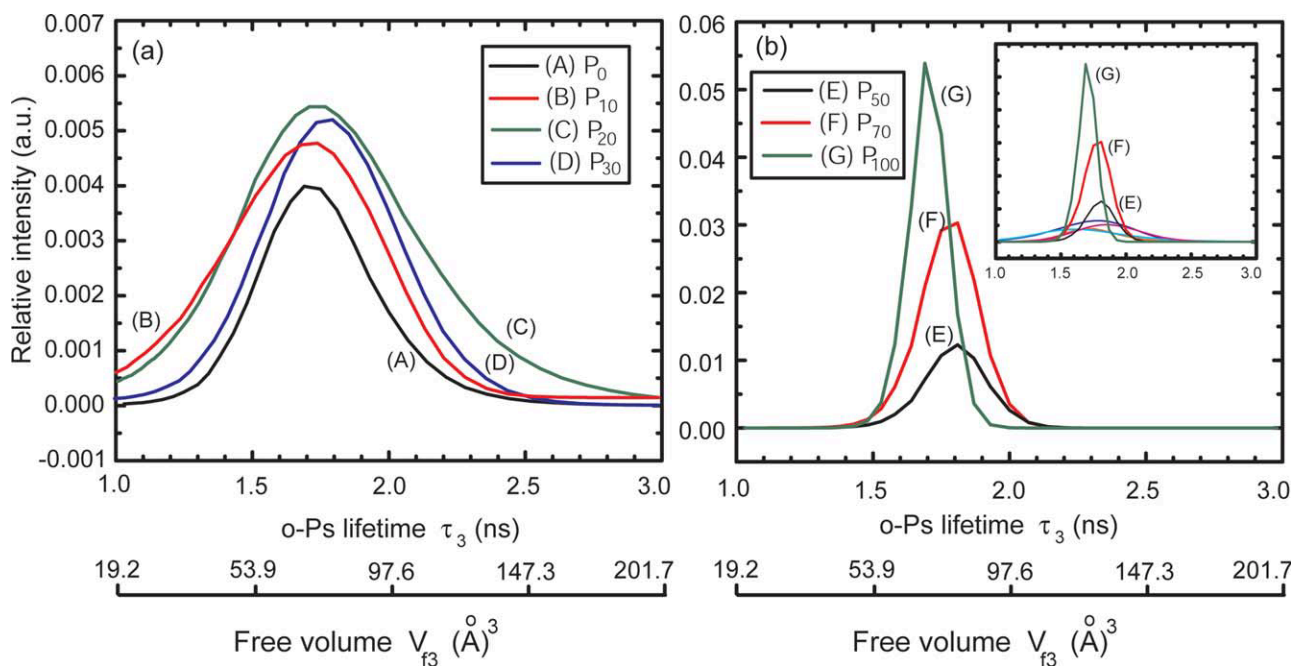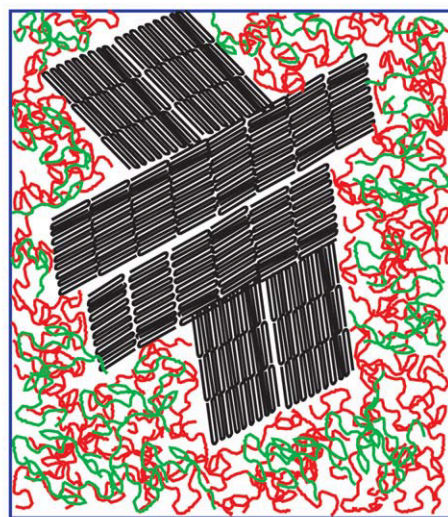
Figure 5 (a) Histograms of o-Ps lifetime distribution plot for samples P_0 (A), P_{10} (B), P_{20} (C), P_{30} (D) while (b) is that for samples P_{50} (E), P_{70} (F), and P_{100} (G). The free volume size evaluated from Tao-Eldrup relation is provided below. The inset in (b) gives the distribution of the entire blend compositions in one glance. [Color figure can be viewed in the online issue, which is available at wileyonlinelibrary.com.]

is a change in the arrangement of amorphous domains that contributes to these free volumes. It is to be recalled here the discussions made under sections MDSC results and Composition dependence of

free volume that at this composition of PEI, the interlamellar segregation of PEI chains in the PEEK lamellar domains starts (see Fig. 6) leading to a possible RAF region.
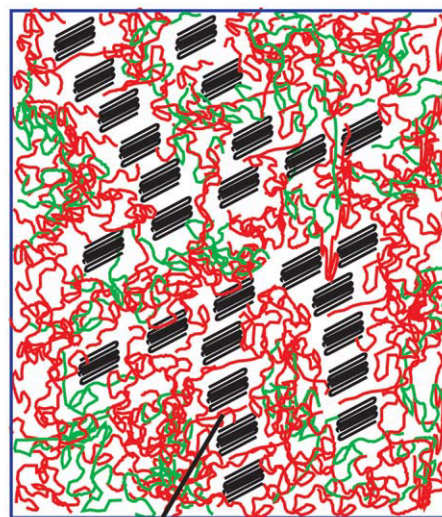
Figure 6 The schematic illustration of arrangement of chains in PEEK/PEI blends (a) when the PEI content is <50% and (b) when the PEI content is ≥50%. [Color figure can be viewed in the online issue, which is available at wileyonlinelibrary.com.]
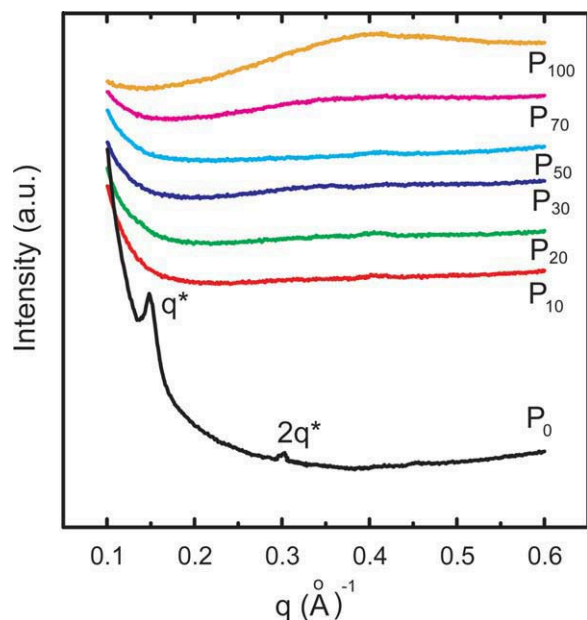
Figure 7 SAXS profiles of PEEK/PEI blend at various compositions. The profiles have been displaced vertically for clarity. [Color figure can be viewed in the online issue, which is available at wileyonlinelibrary.com.]

When a polymer crystallizes, the crystals grow from the individual nuclei. The chains fold and grow in three dimensions to form lamellar structure. It is well established that the free volume cavities are located between polymer chains and at polymer chain ends. Hence, upon interlamellar segregation, the space between the noncrystalline polymer chains gets compressed and so is the associated free volume of the blend leading to a narrow free volume hole distribution. It is to be noted here that in a study on PEO/PMMA blends, Maurer et al., have reported that free volume distributions obtained using MELT program is more powerful to judge the miscibility of the polymer blends compared with conventional thermal analysis techniques like DSC and DMA.[23] So far, the free volume studies on RAF regions have been reported only on semicrystalline polymers.[39,40] For the first time, we report here the influence of interlamellar segregation and the associated formation of RAF regions on the free volume distribution in a polymer blend.

It is appropriate to compare the present results with melt crystallized and rapidly cooled poly (3-hydroxybutyrate-*co*-3-hydroxyvalerate) (PHBV).[24] The authors observed a wider free volume distribution with melt-crystallized PHBV while narrow free volume distribution was noted in rapidly cooled PHBV. The authors have explained that, upon rapid cooling, larger amount of amorphous phase is constrained between the crystalline lamellae that led to narrow free volume distribution,[24] which is in consonance with our results. The arrangement of PEEK and

PEI chains in the blend when the PEI content is <50% and ≥50% are schematically represented in Figure 6.

Small angle X-ray scattering results

To obtain a more detailed picture of the arrangement of PEEK/PEI chains in the blend, the SAXS profiles for PEEK/PEI blends were obtained and the same is presented in Figure 7. Pure PEEK shows a sharp scattering peak at $q = 0.149$ Å^{-1} (first order reflection; where $q = ((4\pi/\lambda) \sin\theta)$ accompanied by a weaker but still clear second-order reflection at $2q$ consistent with the lamellar structure with a periodicity $L(=2\pi/q^*)$ of ~ 42.2 Å. Pure PEI shows a very broad reflection indicating no orderliness of chains, in agreement with its amorphous nature. Surprisingly, even with the little addition of PEI, the scattering peaks vanishes suggesting possible destruction of the lamellar periodicity. Since the densities of PEEK and PEI are very close,[41] could be the reason the SAXS profiles shows no proper indication regarding the finer details of the arrangement of chains. These results are in agreement with the room temperature SAXS pattern reported for this blend.[6]

Wide angle X-ray scattering results

The WAXS profiles for these samples are presented in Figure 8 in the q range 0.5–5.0 Å^{-1} that reflects the overall change in crystalline nature of the PEEK upon PEI addition. Here too, the scattering profile of PEEK shows well defined sharp primary peak with maximum at ca. $q = 1.336$ Å^{-1} accompanied by few satellite peaks in agreement with its crystalline nature. The four distinct peaks observed in the
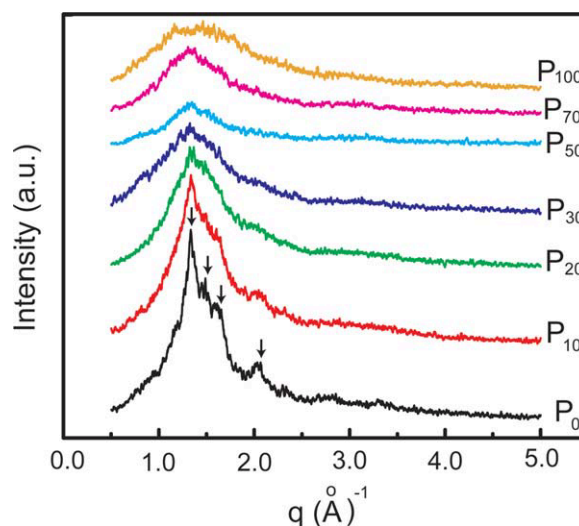

Figure 8 WAXS patterns of PEEK/PEI blend at various compositions. The patterns have been displaced vertically for clarity. [Color figure can be viewed in the online issue, which is available at wileyonlinelibrary.com.]
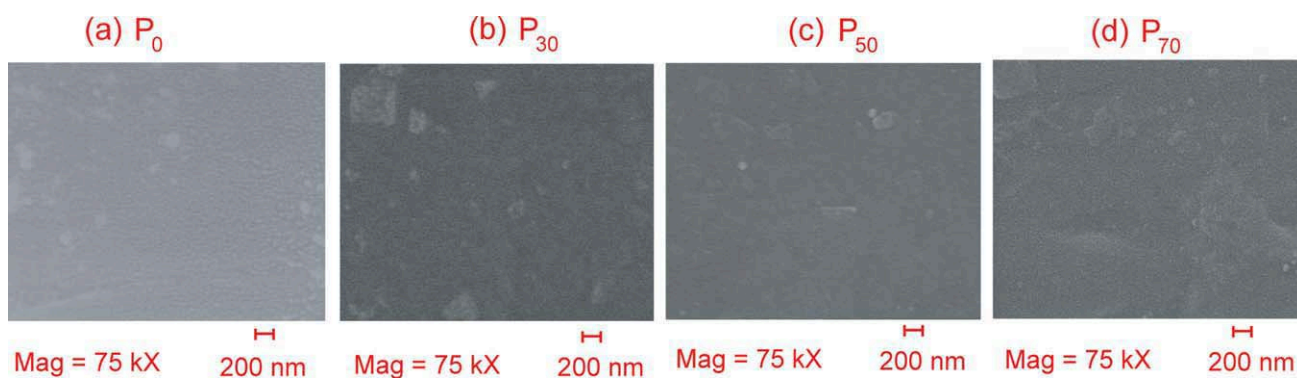
Figure 9 The scanning electron micrographs of PEEK/PEI blend for (a) P_{10}, (b) P_{30}, (c) P_{50}, and (d) P_{70} samples. [Color figure can be viewed in the online issue, which is available at wileyonlinelibrary.com.]

diffractogram of PEEK (marked with arrows in Fig. 8) agrees well with its scattering profile reported.[42] On the other hand, the amorphous PEI exhibits a broad scattering profile centered at around the same q value as that of the primary sharp maximum of PEEK. With the increase in PEI addition, the narrow primary crystalline peak becomes broad and when the PEI content is 50%, the primary peak gets greatly suppressed indicating that there is a significant change in the crystalline/amorphous nature of the blend. This drastic change in crystalline/amorphous nature can be correlated to the formation of inter-lamellar segregation which is also well reflected in the DSC results as the depression in the melting point (T_m)[9] (see Table I). Further addition of PEI leads to broadening of the main peak, due to increase in overall PEI content in the blend.

SEM results

The SEM images of the blends were taken for the samples P_{10}, P_{30}, P_{50}, and P_{70} and are displayed in Figure 9(a–d), all of which taken at a magnification of 75,000×. When the PEI content is <50%, no microphase separation could be detected at least at 200 nm scale or better (please see micrographs for samples P_{10} and P_{30}) as indicated in PALS distribution pattern. The samples with PEI content ≥50% also appear homogeneous (please see micrographs for samples P_{50} and P_{70}). Even a recent work using transmission electron microscope (TEM) on a similar grade of PEEK and PEI also suggests that the blend to be completely homogeneous.[8] Thus, this study reveals the superiority of PALS over the other techniques in understanding the extent of miscibility at the nanoscopic level, at least in this polymer blend.

Correlation between molecular mobility from MDSC and PALS results

Since both the heat capacity and free volume are a measure of molecular mobility,[16,20,43] we have made

an attempt to understand whether there is a correlation between these two parameters. The plot of ΔC_p against F_{vr} is shown in Figure 10. The lower value of ΔC_p indicates lesser molecular mobility.[43] Accordingly, the pure PEEK (sample P_0) having less free volume also exhibits less ΔC_p and with the addition of PEI, the molecular mobility of the blend increases due to increase in amorphous content. Thus, the value of ΔC_p increases with the free volume content in the blend.

In the preparation of high dielectric polymer composites, the presence of nanovoids and interfaces needs to be minimum as the voids decrease the dielectric constant.[44] We believe that the results obtained from this study will be very much useful to select the composition of PEEK and PEI in the preparation of high dielectric materials based on this miscible blend. The free volumes present in the interlamellar regions (RAF) are constituted by the amorphous chains that are constrained and as such their thermal expansion would be different
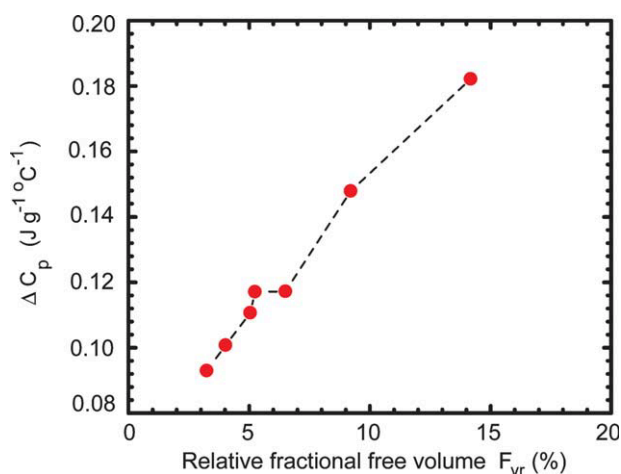

Figure 10 The variation of ΔC_p obtained from MDSC measurements with relative fractional free volume (F_{vr}) evaluated from positron lifetime measurements. [Color figure can be viewed in the online issue, which is available at wileyonlinelibrary.com.]

compared to rest of the amorphous part. A thorough study is on progress to explore the thermal behavior of free volume holes in this blend in terms of mobile and rigid amorphous fractions.

CONCLUSIONS

For the first time, we have used the combined free volume studies and the advanced MDSC in PEEK/ PEI blends to understand the extent of miscibility at the nanoscopic level. On the basis of the results, it is suggested that high degree of miscibility of PEEK/ PEI blend is obtained when the PEI content in the blend is $\geq$50%. At this level of PEI content, the free volume distribution becomes narrow and seems to support the concept of interlamellar segregation of PEI chains. The MDSC results show the possible existence of RAF regions, a fact that is also indicated in the WAXS measurements when the PEI content is 50%, and thus supplements the positron lifetime results. To the best of our knowledge, the influence of interlamellar segregation on the free volume distribution in a polymer blend has never been discussed.

References

1. Harris, J. E.; Robeson, L. M. J Appl Polym Sci 1988, 35, 1877.
2. Crevecoeur, G.; Groeninckx, G. Macromolecules 1991, 24, 1190.
3. Shibata, M.; Fang, Z.; Yosomiya, R. J Appl Polym Sci 2001, 80, 769.
4. Chen, H. L.; Porter, R. S. J Polym Sci Part B Polym Phys 1993, 31, 1845.
5. Goodwin, A. A.; Simon, G. P. Polymer 1996, 37, 991.
6. Jonas, A. M.; Ivanov, D. A.; Yoon, D. Y. Macromolecules 1998, 31, 5352.
7. Ivanov, D. A.; Jonas, A. M. J Polym Sci Part B Polym Phys 1998, 36, 919.
8. Nemoto, T.; Takagi, J.; Ohshima, M. Polym Eng Sci 2010, 50, 2408.
9. Ramani, R.; Alam, S. Thermochim Acta 2010, 511, 179.
10. Wästlund, C.; Berndtsson, H.; Maurer, F. H. J. Macromolecules 1998, 31, 3322.
11. Takegoshi, K.; Tsuchiya, K.; Hikichi, K. Polymer J 1995, 27, 284.
12. Zhao, J.; Ediger, M. D.; Sun, Y.; Yu, L. Macromolecules 2009, 42, 6777.
13. Kammer, H. W.; Kressler, J.; Kummerlöewe, C. Adv Polym Sci 1993, 106, 31.
14. Kong, X.; Narine, S. S. Biomacromolecules 2008, 9, 1424.
15. Patrício, P. S. O.; de Sales, J. A.; Silva, G. G.; Windmöller, D.; Machado, J. C. J Membr Sci 2006, 271, 177.
16. Andersson, A.; Zhai, W.; Yu, J.; He, J.; Maurer, F. H. J. Polymer 2010, 51, 146.
17. Sakaguchi, T.; Taniguchi, N.; Urakawa, O.; Adachi, K. Macromolecules 2005, 38, 422.
18. Hu, X.; Lu, Q.; Sun, L.; Cebe, P.; Wang, X.; Zhang, X.; Kaplan, D. L. Biomacromolecules 2010, 11, 3178.
19. Liu, J.; Jean, Y. C.; Yang, H. Macromolecules 1995, 28, 5774.
20. Jean, Y. C. Microchem J 1990, 42, 72.
21. Ranganathaiah, C.; Kumaraswamy, G. N. J Appl Polym Sci 2009, 111, 577.
22. Zhu, Y.; Wang, B.; Gong, W.; Kong, L.; Jia, Q. Macromolecules 2006, 39, 9441.
23. Wästlund, C.; Maurer, F. H. J. Macromolecules 1997, 30, 5870.
24. Cheng, M. L.; Sun, Y. M. J Polym Sci Part B Polym Phys 2009, 47, 855.
25. Nakanishi, H.; Wang, S. J.; Jean, Y. C. In Positron Annihilation Studies of Fluids; Sharma, S. C., Ed.; World Scientific: Singapore, 1988; p 292.
26. Eastmond, G. C.; Daly, J. H.; McKinnon, A. S.; Pethrick, R. A. Polymer 1999, 40, 3605.
27. Nguyen, H. X.; Ishida, H. Polym Comp 1987, 8, 57.
28. Ramani, R.; Ramachandra, P.; Ramgopal, G.; Ranganathaiah, C. J Appl Polym Sci 1998, 68, 2077.
29. Pethrick, R. A.; Prog Polym Sci 1997, 22, 1.
30. Kirkegaard, P.; Pedersen, N. J.; Eldrup, M. In Riso National Laboratory Report, Denmark, 1989, M-2740.
31. Skukla, A.; Peter, M.; Hoffmann, L. Nucl Instr Meth A 1993, 335, 310.
32. Tao, S. J. J Chem Phys 1972, 56, 5499.
33. Eldrup, M.; Lightbody, D.; Sherwood, J. N. Chem Phys 1981, 63, 51.
34. Lin, J.; Shenogin, S.; Nazarenko, S. Polymer 2002, 43, 4733.
35. Magoń, A.; Pyda, M. Polymer 2009, 50, 3967.
36. Chun, Y.S.; Lee, H.S.; Jung, H.C.; Kim, W.N. J Appl Polym Sci 1999, 72, 733.
37. Hill, A. J.; Zipper, M. D.; Tant, M. R.; Stack, G. M.; Jordan, T. C.; Shultz, A. R. J Phys Cond Matter 1996, 8, 3811.
38. Dlubek, G.; Hübner, C.; Eichler, S. Nucl Instr Meth B 1998, 142, 191.
39. Kilburn, D.; Bamford, D.; Lüpke, T.; Dlubek, G.; Menke, T. J.; Alam, M. A. Polymer 2002, 43, 6973.
40. Cheng, M. L.; Sun, Y. M.; Chen, H.; Jean, Y. C. Polymer 2009, 50, 1957.
41. Hsiao, B. S.; Sauer, B. B. J Polym Sci Part B Polym Phys 1993, 31, 901.
42. Woo, E. M.; Tseng, Y. C. J Polym Sci Part B Polym Phys 1999, 37, 1485.
43. Mohamed, A.; Gordon, S. H.; Biresaw, G. Polym Degrad Stabil 2007, 92, 1177.
44. Maier, G. Prog Polym Sci 2001, 26, 3.